Arsenic, selenium, and mercury speciation in hypersaline lakes of the Andean Altiplano: Link between extreme levels and biodiversity repartition

Stéphane Guédron, Julie Tolu, David Amouroux, Emmanuel Tessier, Carlos Molina, Maïté Bueno, Adrien Mestrot, Delphine Tisserand, Dario Acha

▶ **To cite this version:**

Stéphane Guédron, Julie Tolu, David Amouroux, Emmanuel Tessier, Carlos Molina, et al.. Arsenic, selenium, and mercury speciation in hypersaline lakes of the Andean Altiplano: Link between extreme levels and biodiversity repartition. Journal of Geochemical Exploration, 2024, 267, pp.107577. 10.1016/j.gexplo.2024.107577 . hal-04698703

HAL Id: hal-04698703

https://univ-pau.hal.science/hal-04698703

Submitted on 16 Sep 2024

HAL is a multi-disciplinary open access archive for the deposit and dissemination of scientific research documents, whether they are published or not. The documents may come from teaching and research institutions in France or abroad, or from public or private research centers.

L'archive ouverte pluridisciplinaire **HAL**, est destinée au dépôt et à la diffusion de documents scientifiques de niveau recherche, publiés ou non, émanant des établissements d'enseignement et de recherche français ou étrangers, des laboratoires publics ou privés.

Distributed under a Creative Commons Attribution 4.0 International License

Journal of Geochemical Exploration 267 (2024) 107577

Contents lists available at ScienceDirect

Journal of Geochemical Exploration

journal homepage: www.elsevier.com/locate/gexplo

Arsenic, selenium, and mercury speciation in hypersaline lakes of the Andean Altiplano: Link between extreme levels and biodiversity repartition

Stéphane Guédron [a,*], Julie Tolu [b,c,f], David Amouroux [b], Emmanuel Tessier [b], Carlos Molina [d], Maïté Bueno [b], Adrien Mestrot [d], Delphine Tisserand [a], Dario Acha [e,*]

[a] Univ. Grenoble Alpes, Univ. Savoie Mont Blanc, CNRS, IRD, IFSTTAR, ISTerre, 38000 Grenoble, France
[b] Universite de Pau et des Pays de l'Adour, E2S UPPA, CNRS, IPREM, Institut des Sciences Analytiques et de Physico-chimie pour l'Environnement et les matériaux, Pau, France
[c] Eawag, 8600 Dübendorf, Switzerland
[d] University of Bern, Institute of Geography, CH-3012 Bern, Switzerland
[e] Universidad Mayor de San Andres, Instituto de Ecologia, LCA, La Paz, Bolivia
[f] ETH Zürich, 8092 Zürich, Switzerland

ARTICLE INFO

Keywords:
South Lipez
High altitude lakes
Extreme environment
Sediment
Atmosphere

ABSTRACT

Arsenic (As) and mercury (Hg) are highly toxic contaminants whereas selenium (Se) is both an essential trace element and potentially harmful at higher concentrations. The hyper-saline lakes of southern Bolivian Altiplano, which are ecological niches for endemic species, are also expected to be enriched in these toxic trace elements. The biogeochemistry of As, Hg, and Se in such high-altitude extreme environments (e.g., high UV radiation and salt content) remains poorly understood. In this study, we investigated the concentrations and chemical forms (speciation) of As, Hg, and Se in sediment, water, and air samples of Lagunas Colorada (LC), Verde (LV), and Blanca (LB) in the South Lipez region (>4200 m a.s.l.). We compared them with the repartition of biodiversity (invertebrates, algae, and bacteria). Extreme As concentrations were found in water (up to 82 mg L^{-1}), and the main As species was inorganic As(V), with neither biogenic methylated As nor volatile As forms being detected in water and air, respectively. Se concentrations in water were of 0.1 to 1.4 μg L^{-1}, and Se existed under different redox states, i.e., Se(IV), Se(VI), and reduced Se (0, -II), including biogenic methylated Se(-II) (trimethyl selenonium). Volatile Se compounds (e.g., dimethyl selenide) were detected in water and air samples. Hg was enriched in the surface water (6 to 30 ng L^{-1}) compared to other regional water bodies, and a significant amount of methyl-Hg and gaseous Hg(0) was detected. The drastic disparity between As, Se and Hg concentrations and speciation between lakes has important implications for their cycling in these extreme aquatic systems. While As mostly accumulated in its oxidized and non-volatile form, Hg and Se concentrations can be controlled by significant conversion to reduced and methylated forms, allowing efficient evasion to the atmosphere. Finally, the salinity, including major ions, and high levels of As were among the main drivers of biodiversity repartition between lakes.

1. Introduction

The concentrations and chemical forms (speciation) of trace elements in the environment are key factors for human health and the functioning of ecosystems. Arsenic (As) and mercury (Hg) are two highly toxic elements for humans, animals, and microorganisms (Bissen and Frimmel, 2003; Chang, 1977; Dopp et al., 2004; Gadd, 1993). In contrast, selenium (Se) is an essential trace element for humans and (micro)organisms that can be a potential antagonist of As and Hg toxicity depending on its speciation (Wang et al., 2004). At elevated concentrations, Se can, however, be toxic, and elevated waterborne Se concentrations represent an environmental problem in some aquatic ecosystems, such as the Kesterson Reservoir in California (Maier and Knight, 1994). The toxicity of As, Hg, and Se in water depends on, not only their concentrations, but also their speciation, with trivalent As [i.e., arsenite (As(III))] compounds, selenomethionine (SeMet), selenite [Se(VI)], and selenate [Se(IV)], and Hg methylated forms [i.e., monomethylmercury (MMHg)] being the most toxic species of As, Se and

* Corresponding authors.
E-mail addresses: stephane.guedron@ird.fr (S. Guédron), darioacha@yahoo.ca (D. Acha).

https://doi.org/10.1016/j.gexplo.2024.107577
Received 15 February 2024; Received in revised form 26 July 2024; Accepted 31 August 2024
Available online 3 September 2024
0375-6742/© 2024 The Authors. Published by Elsevier B.V. This is an open access article under the CC BY license (http://creativecommons.org/licenses/by/4.0/).

Hg (Clarkson and Magos, 2006; Duker et al., 2005; Rohn et al., 2018). Hence, understanding the distribution and chemical forms of trace elements in the environment is important in assessing human health, biodiversity, and ecosystem functioning (Maier and Knight, 1994; Mandal and Suzuki, 2002; Zwolak and Zaporowska, 2012).

Volcanic regions are geologically enriched in As, Hg, and Se and thus play a particular role in local (i.e., catchment) and/or regional wildlife and biodiversity. These regions are also important at larger scales as they represent an important source of these elements to the global atmosphere (Floor and Román-Ross, 2012; Nriagu and Becker, 2003; Tapia et al., 2019). As, Se and Hg are naturally released into the environment from geogenic sources including volcanic rocks, atmospheric emissions (gas and volcanic ashes), and geothermal fluids ascending from deep geothermal reservoirs (Bagnato et al., 2014; Bundschuh et al., 2020). This is the case in the high-altitude aquatic ecosystems (above 3500 m a.s.l.) of the south-central Andean Altiplano, where high geogenic As levels ranging between 5.2 and 250 μg L^{-1} have been reported in ground and surface waters, originating primarily from the alteration of volcanic rocks and re-dissolution of ancient evaporites (Ormachea Munoz et al., 2013; Ramos Ramos et al., 2012; Ramos Ramos et al., 2014; Sarret et al., 2019; Tapia et al., 2019). Such high As levels are critical for wildlife and humans, with regional As-related adverse human health effects for the local population reported for at least 7000 years (Arriaza et al., 2009; De Loma et al., 2019). However, with the exception of some investigations on total As concentrations (Figueroa, 2018), the speciation and biogeochemistry of redox reactive and volatile trace elements such as As, Hg, and Se have never been studied jointly in such extreme environments.

In the South Lipez region, one of the driest cold deserts in the world, the extreme salinity and insolation impairing the ability of microbial organisms to repair DNA (Cockell, 2001), has resulted in singular adaptations of biological life, as revealed by the identification of new species of nitrogen-fixing cyanobacteria and completely novel taxa unrelated to any known cyanobacteria (Fleming and Prufert-Bebout, 2010). In addition, because of the singularity of this extreme environment (i.e., low average temperature, high-daily temperature amplitude, high-UV radiation, ice, reduced yearly precipitation, volcanic and hydrothermal environment), it has been chosen as an analog to study the putative life in early Martian lakes (Cabrol et al., 2009). Apart from the bright colors from which their names come from, these lakes constitute a unique ecological niche for endemic flora and fauna, including migratory water bird species (Caziani et al., 2001; Lopez and Zambrana-Torrelio, 2006; Williams et al., 1995), which makes them a very popular place for tourism. However, there is a great biodiversity disparity between the different lakes, which could result from contrasted geochemical context, particularly associated with the relative abundance of contaminants such as As and Hg versus beneficial micronutrients such as Se.

In this study, we investigated the concentration and speciation of As, Hg, and Se in three saline lakes in the South Lipez region (i.e., Laguna Colorada, Verde, and Blanca). Our exploration was conducted in and between the different compartments of these aquatic systems, i.e., the sediment, the water column, the atmosphere, and biomats to document Hg, As, and Se biogeochemical behavior in these extreme aquatic environments. Finally, we conducted a preliminary biodiversity inventory (invertebrates, algae, and bacteria) of these lakes and related them to environmental parameters, including levels of major and trace elements. Our hypothesis was that expected high concentrations of As, Hg and/or Se in the saline lakes of the South Lipez region may influence (micro) organisms abundance and biodiversity because of their toxicity and/or essentiality for (micro)organisms.

2. Material and methods

2.1. Environmental settings and sampling locations

The large endorheic Altiplano basin located between the Oriental and Occidental Cordilleras of the tropical Andes encompasses both the world's largest high-altitude lake (Lake Titicaca) in the seasonally wet northern Altiplano and the large salt flats (Salars de Uyuni and Coipasa) in the arid southern Altiplano (Fig. 1). Located in the southern part of the Bolivian Altiplano, the South Lipez region (21 to 23° S) is a basaltic-andesite environment with numerous shallow and saline lakes mostly fed by volcanic hydrothermal settings (Figueroa, 2018) and weakly precipitations (3 to 60 mm y^{-1}). These high-altitude aquatic ecosystems are temporary or permanent but always subject to wide variations in area. Several prospections performed in the 1970s and 1980s have briefly described and documented their ecology and basic physicochemistry (Hurlbert and Chang, 1988; Risacher and Fritz, 1992; Risacher and Fritz, 1991; Servant-Vildary et al., 2002). Three salt lakes were sampled in this area (Fig. 1). To the North, Laguna Colorada (LC: 22°11′55″S 67°46′52″W, 4298 m asl, ~60 km^2 in surface, 0.35 m depth in average) is composed of brackish waters colonized by algae (mainly flagellate *Dunaliella salina*) and mud Islands [Fig. 1a, (Hurlbert and Chang, 1984)]. Due to massive phytoplanktonic development, the transparency is only a few centimeters (Iltis et al., 1984). A great diversity of avifauna feeds in this water, including Chilean flamingos (Hurlbert et al., 1986).

In the South, Lagunas Verde and Blanca (4328 m asl, Fig. 1b) are two shallow (<0.5 m depth on average) and saline lakes located at the foot of the Licancabur volcano (5920 m asl). Laguna Blanca (LB: 22.800°S 67.794°W; ~11 km^2 in surface) is white and is separated from Laguna Verde (LV: 22°47′38″S 67°48′44″W; ~5.2 km^2 in surface) by a narrow isthmus. Numerous water birds and invertebrates occupy LB, whereas LV is exempt from fauna (Hurlbert and Keith, 1979). Finally, samples were also collected at Titicaca Lake (LT: 16°12′41″S 68°45′57″W), which was only used as a reference for biodiversity comparison.

2.2. Sample collection and conditioning

All samples were collected during a field sampling campaign in April 2016 (from 27th to 29th).

2.2.1. Water

All water samples were collected following ultra-clean techniques and published protocols (Guédron et al., 2017a), and 7 sub-samples were taken to analyze the concentrations of: 1) filtered major anions, 2) dissolved organic carbon (DOC); 3) unfiltered (UNF) total Hg (noted THg_{UNF}) and Hg species; 4) filtered (F) total Hg (noted THg_F); 5) unfiltered As, Se, and other trace and major elements; 6) filtered As, Se and other elements as well as As species; 7) filtered Se species; and 8) volatile As, Hg and Se species. All samples were stored at 4 °C until analysis except for sub-samples 1 (anions), which were collected in 15 mL polyethylene trace grade falcon tubes and frozen within an hour after collection. The sub-samples 2 (DOC) were collected in pre-burnt (550 °C) amber borosilicate vials, acidified with HCl (0.5 %, v/v, Ultrex grade - JT Baker). The sub-samples 3 (THg_{UNF} and Hg_{UNF} species) and 4 (THg_F) were collected respectively in 250 mL and 30 mL acid-washed FEP Teflon containers and acidified with HCl (0.5 %, v/v, Ultrex grade - JT Baker). The sub-samples 5 (unfiltered As, Se, and other elements) and 6 (filtered As, Se, and other elements and As species) were collected respectively in 50 mL and 15 mL PVDF trace-grade falcon tubes and acidified with HNO_3 (2 %, v/v, Ultrex grade - JT Baker). The sub-samples 7 (Se species) were filtered at 0.22 μm (PVDF syringe filters), collected in 15 mL PVDF trace-grade falcon tubes without leaving headspace, and stored frozen within an hour after collection to avoid bacteria activity and thus biological transformation of Se species. Indeed, acidification with HCl or HNO_3 cannot be performed as for Hg

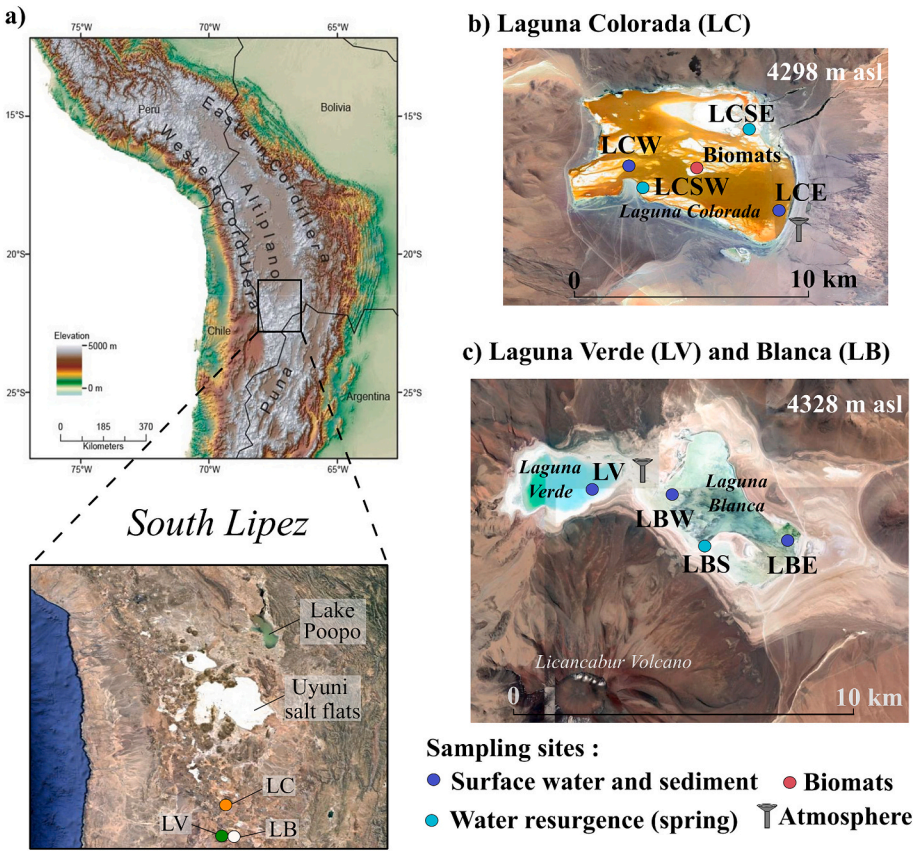

Fig. 1. a) The location of the South Lipez region in the Bolivian Altiplano and of the three salt lakes studied. Sampling locations for surface water, sediment, biomats and atmosphere in b) Laguna Colorada (LC) and c) Laguna Blanca (LB) and Laguna Verde (LB). Letters W, and E refer to the west and east position of sampling location, and letter S to spring. Aerial image modified from Google Earth.

and As speciation sub-sample (see below), because this leads to Se species transformation. For the other filtered sub-samples, filtrations were performed with 0.45 μm (PVDF syringe filters). Finally, the sub-samples 8 (volatile Hg and Se speciation) were collected without headspace in 500 mL FEP acid-washed bottles, subsequently connected to a two-way transfer closure equipped with a Teflon frit, allowing purging of the gaseous species under a controlled N_2 gas flow (500 mL min^{-1}, during 30 min). Dissolved gaseous mercury (DGM) was thus collected on gold-coated sand traps (Brooks Rand), whereas dimethylmercury (DMHg) and Se volatile compounds were trapped on graphitized carbon (Carbotrap®, Supelco) packed columns. All adsorbent traps have been thermodesorbed, sealed with Teflon caps, and stored under a laminar flow hood before use. The purge and trap setup and the operating conditions are described in detail elsewhere (Lanceleur et al., 2019; Duval et al., 2023; Kleindienst et al., 2023).

2.2.2. Sediments and algal biomats

Surface sediment at LC and LB was collected using a UWITEC gravity corer equipped with a 90 mm PVC tube and sliced as described elsewhere (Guédron et al., 2017b). After slicing, the sediments were transferred to a zip bag and were kept frozen until being freeze-dried in the laboratory. In LC, algal biomats were collected at the surface of sediments in zip bags with a plastic spoon and kept frozen until being freeze-dried in the laboratory. All solid samples (sediments and algal biomats) were then freeze-dried and crushed to obtain a fine powder (smaller than 63 mm) for all chemical analyses.

2.2.3. Air

Volatile As species were trapped from the air using a chemotrapping technique following published protocols (Mestrot et al., 2011; Mestrot et al., 2009; Müller et al., 2022; Tessier et al., 2002). Briefly, volatile As species present in the atmosphere were preconcentrated on silver nitrate impregnated (1 % w/v $AgNO_3$) chemotrapping tubes (ref. 226–10, SKC Ltd. Dorset, UK), which contained silica gel and glass wool (Mestrot et al., 2009). Silver-nitrate-impregnated silica gel from the traps was stored at 4 °C until analysis in the lab.

Total Gaseous Hg (TGM) and volatile Se species were trapped from the air by pumping through an online quartz fiber filter (0.1 μm, Whatmann) at a regulated flow rate of 500 mL min^{-1} during 1 h, according to published operating protocols (Amouroux et al., 1998; Amouroux et al., 1999; Bouchet et al., 2011). The adsorbent traps used were similar to those operated for the collection of the dissolved gaseous Hg and Se species, as described above. No moisture trap was installed on the sampling line due to the short sampling duration (ca. 1 h) and the low relative humidity recorded in the air (ca. 20 % and 30 % on daily average for LC and LB/LV, respectively). A portable weather station (Kestrel 4000) was also deployed at 2 m height during the sampling operations to record the basic meteorological parameters needed for the water/air exchange assessment (air temperature and relative humidity, wind speed, and wind direction).

2.3. Measurement methods

2.3.1. General physico-chemical analysis of water and sediment

The water column physico-chemistry (pH, conductivity, salinity, electrical conductivity, salinity, and temperature) was characterized on-site using a submersible multiparameter probe (HANNA HI-9828; Hanna Instruments, Woonsocket, RI, USA) immersed in the surface water.

Anions and cations (ammonium, nitrate, chloride, sulfate, phosphate) were measured by ionic chromatography using a 332 Metrohm

apparatus. Accuracy was evaluated with the Carl Roth 2668.1 standard. Samples with elevated dissolved salts were diluted before measurements. Calcium (Ca), potassium (K), magnesium (Mg) and sodium (Na) were measured by ICP-AOS (Varian model 720ES) within the analytical chemistry platform of ISTerre (OSUG-France).

DOC concentrations were determined using a Non-Dispersive Infra-Red (NDIR) CO_2 Shimadzu® (Kyoto, Japan) (Model VCSN) spectrometer after wet oxidation in a sodium persulfate solution at 100 °C within the Geochemistry and Mineralogy platform at ISTerre. Total organic carbon (C_{org}) and total carbon [from which carbonate content was calculated, (Guédron et al., 2023)] were quantified by Cavity Ring-Down Spectrometer (Picarro, Inc.®) coupled with Combustion Module (Costech, Inc.®) (CM-CRDS) using previously reported analytical methods, calibration, and sample preparation (Heredia et al., 2022).

Acid volatile sulfides (AVS) in surface sediment were measured using a purge and trap system (Tisserand et al., 2021) and analyzed following the methylene blue (MB) method (Cline, 1969). Simultaneously extracted metals (Al, Fe, Mn, Zn, As, Li, and Si) were then measured from the extraction solution by ICP-AOS (Varian model 720ES) within the analytical chemistry platform of ISTerre (OSUG-France).

2.3.2. Elemental quantification and speciation analyses in liquid and solid phases

Total Hg concentrations in filtered (THg_F) and unfiltered (THg_{UNF}) surface water were determined by cold vapor atomic fluorescence spectrometry (CV-AFS) after conversion of all Hg species into Hg0 followed by detection using a Tekran® [Model 2500 (Guédron et al., 2017a; Guédron et al., 2014)]. THg in solid samples was determined by combustion and atomic absorption spectrophotometry using an AMA 254 analyzer (Altec), following the procedure described elsewhere (Guédron et al., 2021). All Hg CRMs data are provided in Table S1. Total As, Se, and other trace elements (i.e., boron (B), bromine (Br), cadmium (Cd), copper (Cu), lithium (Li), manganese (Mn), and antimony (Sb)) were quantified by inductively coupled plasma mass spectrometry (ICP-MS) in filtered waters directly (sub-sample 6), in unfiltered waters (sub-sample 5) after their digestion (HNO_3/H_2O_2), and in sediments and biofilms after acid extraction. Detailed information, including QA/QC, is provided in S.I.1.a and Table S2.

2.3.3. Hg, As, and Se speciation in liquid, solid, and gas phases

Dissolved non-volatile mercury species, including inorganic Hg (Hg (II)) and monomethyl-Hg (MMHg), were analyzed in unfiltered water samples, and microwave digested solids (HNO_3, 6 N solution) by species-specific isotope dilution after derivatization by propylation and detection by Gas Chromatography coupled to an inductively plasma mass spectrometry (GC-ICPMS) (Alanoca et al., 2016a; Monperrus et al., 2008; Monperrus et al., 2005). Dissolved non-volatile As and Se species were analyzed in filtered waters (sub-samples 6 and 7, respectively) using HPLC-ICP-MS coupling and following previously published methods (Chen et al., 2013; Roulier et al., 2021). For As, targeted species were arsenate (AsO_4^{3-}(V)), arsenite (AsO_3^{3-}(V)), monomethyl-arsenate (MMAs), and dimethyl-arsenate (DMAs). For Se, targeted species were Se oxyanions, i.e., selenate (SeO_4^{2-}(IV)) and selenite (SeO_3^{2-}(VI)), seleno-amino acids (i.e., seleno-methionine and seleno-cystine; Se(-II)), and trimethylselenonium ion ($TMSe^{+}$(-II)). As a fraction of Se is known to not elute out of used (and other existing) chromatographic separation, likely corresponding to a reduced Se pool (Red.Se) (Roulier et al., 2021), we estimated the reduced Se (Red.Se) pool as the difference between total Se concentrations and the concentrations of detected Se species. In samples that did not contain quantifiable Se oxyanions species, one-half of their quantification limit (with 100 % associated error) was used to calculate the Red.Se pool. Further details on the used methods, including QA/QC, are provided in S.I.1.b, S.I.1.c and Table S3.

Gaseous Hg species (DGM, TGM, DMHg) as well as Se species (DMSe, DMDSe, and DMSeS) in atmosphere and water samples were analyzed after thermodesorption of their respective adsorbent traps, i.e., by CV-AFS for DGM and TGM and by Cryo-focusing GC-ICPMS, for DMHg and volatile Se species, following published protocols (Alanoca et al., 2016a; Bouchet et al., 2022; Kleindienst et al., 2023; Lanceleur et al., 2019). No DMHg was detected in the analyzed samples, hence DGM and TGM are essentially constituted of dissolved elemental Hg (Hg0). To analyze the gaseous As species trapped on-site from the air, the silver-nitrate impregnated silica gel from the traps was microwave-extracted with 4.8 mL of 1 % (v/v) HNO_3 and 0.2 mL of 30 % (v/v) H_2O_2 using a MARS 6 microwave (CEM, Matthews, NC, USA) (Müller et al., 2022), and total As concentration in the extracts was determined by ICP-MS.

2.3.4. Water-air gas exchange calculations

The exchange fluxes of gaseous As, Hg, and Se species across the water-air interface of the 3 lakes were assessed as described in Duval et al. (2023) and Sharif et al. (2013). The flux densities (FD) calculations were derived from the Fick's Law diffusion model and based on the saturation ratio, the difference between dissolved and atmospheric concentrations, and wind speed. The transfer velocity calculations for the volatile analytes at the water-air interface were adapted from the Nightingale et al. (2000) model and according to the specific in situ water temperature and salinity conditions. The unique characteristics of the studied sites (high altitude non-sheltered shallow lakes exposed to intense wind regime) justified this latter choice, assuming that the gas exchange is mainly driven by the wind speed, generating turbulences at the lake surface. Thus, the FD were calculated using the following equations [example given for Hg species with dissolved gaseous Hg (DGM) and total gaseous Hg in air (TGM)]:

$$FD = k \times \left(DGM - \frac{TGM}{H} \right)$$

$$k = \left(0.222 \times U_{10}^2 + 0.333 \times U_{10}\right) \times \left({S_c\ Hg}/{S_c\ CO_2} \right)^{-0.5},$$

where k is the gaseous Hg transfer velocity (cm h^{-1}) at the water-air interface and H its dimensionless Henry's law constant. U_{10} is the wind speed at 10 m height, derived from field recording at 2 m height and corrected using the Schwarzenbach et al. (2016) equation. S_c represents the Schmidt number of the target volatile species corrected for in situ salinity and temperature conditions.

2.3.5. Benthic macroinvertebrates

Due to the large heterogeneity of sediment granulometry between lakes, the benthic zone was sampled with the kick net method to recover macroinvertebrates. These qualitative samples were preserved in the field with 96° alcohol and sorted in the laboratory under a microscope (Wild 10×). Macroinvertebrate identification was performed by morphoanatomical shape recognition following systematic keys (Domínguez and Fernández, 2009; Merritt and Cummins, 1996).

2.3.6. Algae sampling and identification

Superficial water samples were collected in 500 mL wide-mouth Nalgene® pre-clean flasks and preserved with 5 % Lugol in the dark until analysis. Once at the laboratory, algae were pre-concentrated by centrifugation at 6000 rpm for 5 min. Identification and quantification were conducted with a light microscope in a Neubauer plate using identification keys (Bourrelly, 1966; Wehr, 2003) and visual comparison (Díaz and Maidana, 2005; Entwisle et al., 1997).

2.3.7. Microbial community evaluation

A sediment subsample was collected into sterile DNAase-free 2.5 mL cryogenic tubes during sediment core processing in situ. No neighboring samples were considered to prevent cross-contamination, and sampling devices were sterilized between samples. Collected samples were stored in liquid nitrogen for transport. Samples were then freeze-dried at −50 °C to be later shipped to Omega Bioservices (Norcross, Georgia,

US), where DNA was purified using Soil DNA Kit (Omega Bio-Tek) for later metagenomics16S sequencing in a MiSeq platform (Illumina, Inc.) with primers for V3 V4 region (Klindworth et al., 2013). Sequences were analyzed using an open reference UCLUST pipeline using EzBioCloud (Yoon et al., 2017). Again, using available pipelines in EzBioCloud (Yoon et al., 2017), samples from each lake were grouped for functional markers comparison (Segata et al., 2011). Further analysis and graphics with taxonomic groups and functional markers were conducted using PAST 4 software (Hammer et al., 2001).

2.3.8. Statistical analysis

Correlation and regression analyses were used to evaluate the covariance and the nature of the relationships between abiotic variables and between biological and abiotic variables. Biodiversity was evaluated by considering richness at different taxonomic levels and different indicators of biodiversity such as Phylogenetic diversity (Faith, 1992). The diversity between locations was evaluated with one-way ANOVA and all pairwise multiple comparisons with the Turkey test. Given the number of variables and the nature of the biodiversity variables, multivariate principal component analysis was employed, together with canonical correspondence analysis using Past 4.03 (Hammer and Harper, 2001).

3. Results and discussion

3.1. Physico-chemistry of South Lipez hypersaline lake waters

Surface water temperature in the three studied saline lakes ranged between 0 and 9 °C during the sampling period (April 27th to 29th 2016), reflecting the high temperature fluctuations (−25 °C to +13 °C) at this altitude (Cabrol et al., 2009). The lake waters were all alkaline (pH 7.6 to 8.6, Table 1) as in other high-altitude lakes of the Altiplano [e.g., Lakes Titicaca and Uru-Uru; pH = 8.5 ± 0.6 (Achá et al., 2018; Alanoca et al., 2016b)]. Electric conductivity was high and increased from Laguna Blanca (LB, 29 ± 7 mS cm^{-1}) to Laguna Colorada (LC, 192 ± 37 mS cm^{-1}) and Laguna Verde (LV, 1128 ± 32 mS cm^{-1}). The high salinity of the lake waters results from low precipitation and high evaporation occurring in the study region at this altitude, which concentrates ions such as halogens, alkali and alkaline-earth metals in water (Table S4). Dissolved salts were mainly dominated by B, Li, Cl, Br, and sulfates in the 3 lakes (Table S4). Average phosphate, nitrite, and sulfate concentrations were also elevated and typical of volcanogenic emissions of nutrients into groundwater (Jones and Gislason, 2008). The large variability in salinity between the three lakes results from the dilution of endorheic waters with spring waters. Indeed, the conductivity of two monitored spring waters (LCSE and LCSW, Table 1) going into LC was at least 100 times lower than the one of the lake itself, in agreement with data reported in the late 80's (Scandiffio and Alvarez, 1992).

The large number of springs on the eastern side of LB also explains the differences in salinity between LB and the adjacent LV, which does not receive any spring waters (Cabrol et al., 2009; Hurlbert and Keith, 1979). Surface sediment composition (Table S5) also reflects the overall high salinity, with carbonate content increasing from ~30 % at LC to >85 % at LV. In contrast, organic carbon (C_{org}) decreased from LC (C_{org} = 1.2 %) to LB (0.9 %) and LV (0.3 %). In surface water, the highest DOC content was consistently found at LC. Still, DOC was higher in LV than LB (Table S4). Such a trend probably results from enhanced organic carbon preservation in high salinity lakes resulting from lower bacterial activity and weaker OM recycling by organisms (Jellison et al., 1996).

3.2. Biodiversity repartition between lakes

The pelagic and benthic repartition of invertebrates, algae, and bacteria provides a glimpse into the differences in biodiversity and abundance of genera or species in the 3 studied lakes. Benthic invertebrate taxa (Fig. 2 and Table S6) decreased with increasing salinity in surface water from LB to LC, and no invertebrates could be identified in LV. Taxa and taxa numbers were consistent with previous studies performed in the region (Williams et al., 1995) and highlighted that these hypersaline lakes are at least 3 times more impoverished in diversity compared to the slightly saline Lake Titicaca (MMAyA, 2016). Although salinity at LC has increased by a factor of 2 since 1987 (Dejoux, 1993), this does not seem to have impacted the diversity.

The highest algal (Fig. 3a) and bacterial (Fig. 3b and c) diversity in surface water and sediment were found in Lake Titicaca (LT) and LB, whereas the lowest was found in LC and LV ($p < 0.05$). Bacterial phylogenetic diversity was significantly higher at LT than at LB ($p < 0.004$) and LC ($p < 0.006$). Shannon and Chao diversity indexes also showed a significant difference between LT and LB or LC ($p < 0.001$) but were not significant between LB and LC ($p = 0.052$ and 0.076

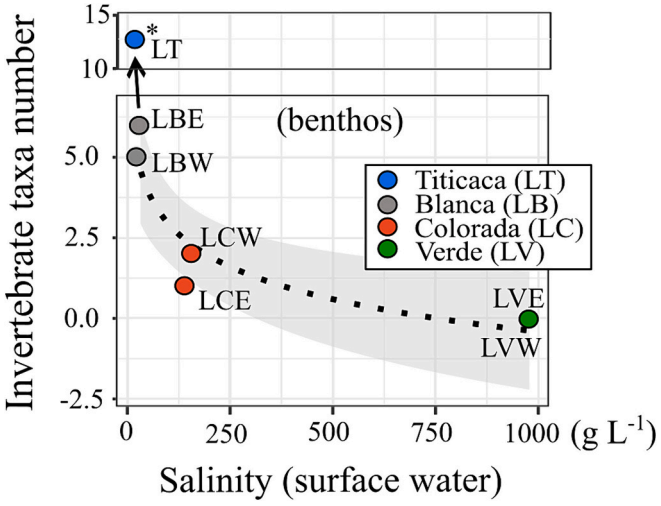

Fig. 2. Biplots of the number of invertebrate taxa identified in surface sediment versus lake salinity for samples collected in Laguna Blanca (LB), Laguna Colorada (LC), Laguna Verde (LV), and Lake Titicaca (LT). *Data for Lake Titicaca are taken from the literature (MMAyA, 2016).

Table 1
Physico-chemical parameters [temperature (Temp.), electrical conductivity (EC.), pH, and redox potential (Eh)] for the Laguna Colorada (4298 m a.s.l.) and two of its springs, the Laguna Blanca (4328 m a.s.l.) and the Laguna Verde (4328 m a.s.l.) measured with a multiparameter Hanna probe. N.A. refers to not analyzed samples.

Location	Sampling site	GPS coordinates	Sampling date (time)	Temp. (°C)	EC (mS cm^{-1})	pH	Eh (mV)
Laguna Colorada	LCW	S 22°12.720′ W67°47.897′	04/27/2016 (07:00)	2	165.2	8.5	−135
	LCW	S 22°12.753′ W67°48.200′	04/27/2016 (13:22)	9.6	182.5	8.1	−118.1
	LCE	S 22°13.160′ W67°44.007′	04/27/2016 (17:53)	N.A.	172.8	8.1	N.A.
	LCE	S 22°13.160′ W67°44.007′	04/28/2016 (10:01)	N.A.	246.2	N.A.	N.A.
	LCSE	S 22°12.786′ W67°47.863′	04/27/2016 (11:43)	29.8	1.3	6.9	−69.5
	LCSW	S 22° 12.928′ W 67° 47.762′	04/27/2016 (14:00)	20.9	1.4	8.4	−115.5
Laguna Blanca	LBE	S 22°48′4.26″ W67°48′1.99″	04/28/2016 (11:34)	0.3	34.5	8.6	−85
	LBW	S 22°49.269′ W67°47.245′	04/28/2016 (14:00)	N.A.	24.0	8.4	−80
Laguna Verde	LVE	S 22°47′54″ W67°49′471″	04/29/2016 (14:00)	N.A.	1150	7.6	N.A.

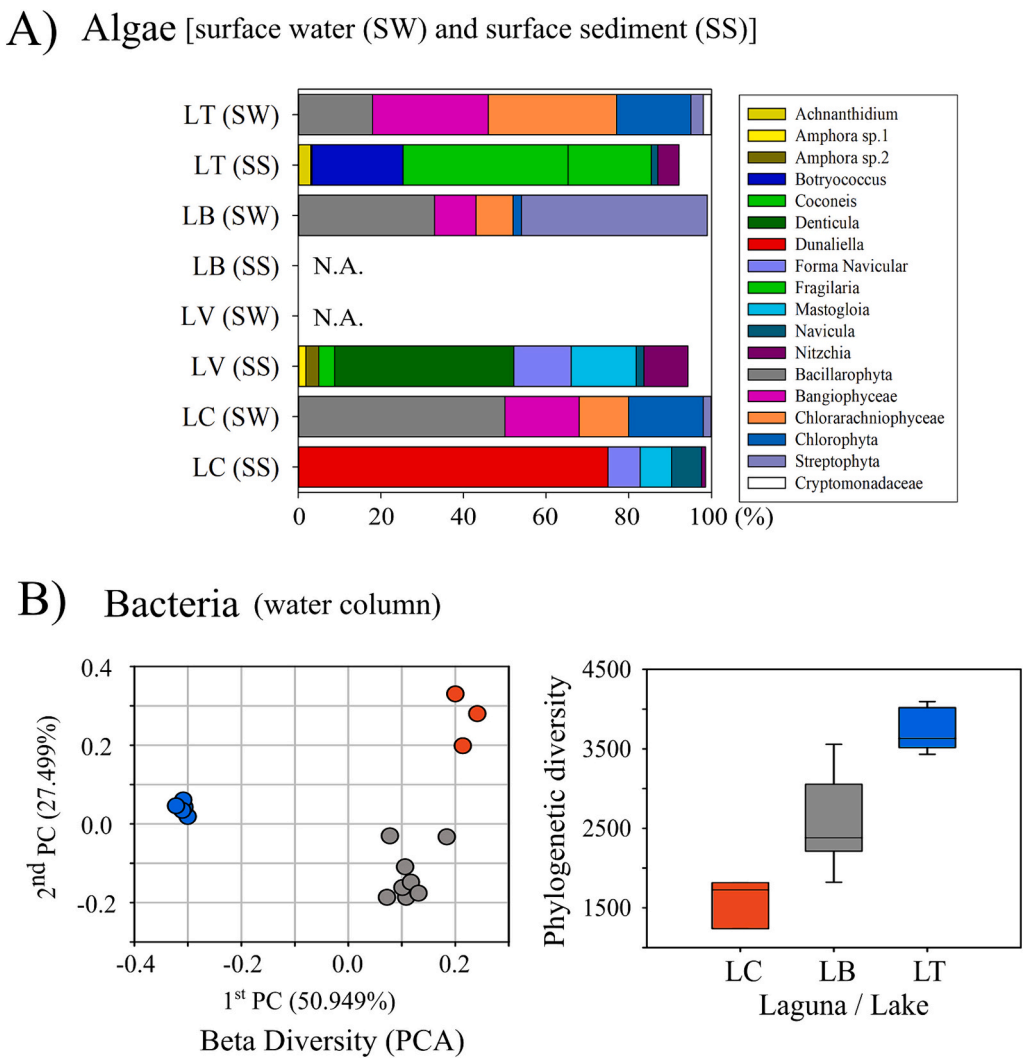

Fig. 3. Representation of the general algal and bacterial biodiversity for samples collected in Laguna Blanca (LB), Laguna Colorada (LC), Laguna Verde (LV), and Lake Titicaca (LT).
a) relative abundance of the main algal genus (with abundance >3 %) identified optically (microscope identification and counting) in surface water (SW) and by e-DNA in surface sediment (SS). The complete list of genera is provided in Table S7. b) Principal component analysis (PCA) of bacterial Beta diversity (left) and phylogenetic diversity of identified bacteria in surface sediments (right). N.A. indicates not analyzed samples.

respectively), which probably reflects on the magnitude of the differences both in biodiversity as well as in the metal and metalloid concentrations.

The diversity of algae in LV could be overestimated. No significant amounts of DNA could be extracted from LV samples, explaining the lack of bacterial diversity data. The algae in LV may not be active or alive but could result from dead algae transported from dust or nearby LB. All algae found in LV are diatoms, which could be long dead and still identifiable because of their valves. Such a group is also frequent in soils and temporary ponds (Pfister et al., 2017). The green algae *Dunaliella salina* dominated the algal community (up to 75 %) at LC, which is consistent with findings in similar environments of the region (Angel et al., 2016). Likewise, the green algae *Streptophyta* was the most abundant at LB, which agrees with Charophyte green algae being highly tolerant to extreme conditions such as intense light radiation (Holzinger and Pichrtová, 2016). However, diatoms are also important at LB, which is unsurprising since this group is known to be abundant in such extreme environments (Angel et al., 2016; Cadima et al., 2005).

Hence, although LC is the likely most productive lake according to its high content in suspended solids and OM content in the sediments, the highest algal and bacterial biodiversity (i.e., beta and phylogenetic diversities) were found in LB surface water and sediments and sharply decreased in LC and LV. The higher productivity at LC seems primarily related to higher algae abundance, which may be explained by higher temperatures than at LB (Table 1), sustained by more abundant hot springs. On the contrary, lower diversity at LC than at LB seems to be driven by higher salinity (Fig. S1), which favors the predominance of a few highly specialized species (e.g., Dunaliella). The less saline LB favors higher diversity with more diverse algae and bacteria with intermediate tolerance to salinity. In the case of LV, salinity and metal concentrations may be too high to allow significant or detectable amounts of life by the means employed here.

3.3. *Extreme arsenic content in lake water and sediment*

The total arsenic concentration in surface waters ranged between ~8 and ~80 mg L^{-1}, with 81 to 100 % of total As found in the dissolved fraction (Table 2). As was found entirely in the form of arsenate (As(V)) at LV and LB, and As(V) represented between 57 and 100 % of TAs at LC (Table 2). Hence, the reduction of As(V) to As(III) mainly occurred in the eutrophic lake LC, and was negligible in the more oligotrophic lakes LV and LB. Consistently with the peculiar geochemical conditions of such

Table 2
Total arsenic concentrations in filtered (F) and unfiltered (UNF) surface waters and arsenic speciation in filtered surface waters of the three studied saline lakes.

Location	Sampling site	TAs_{UNF} (mg L^{-1})	TAs_F (mg L^{-1})	As (III) (mg L^{-1})	As (V) (mg L^{-1})	As (V) %TAs
Laguna Verde	LVE	68 ± 4	72 ± 9	1.1 ± 0.2	81 ± 1	113 ± 14
Laguna Colorada	LCE	79 ± 2	84 ± 11	17 ± 1	78 ± 3	93 ± 6
	LCW	77 ± 3	N.A.	6.4 ± 0.2	87 ± 1	112 ± 4
Laguna Blanca	LBE	9.2 ± 0.6	10.2 ± 0.9	0.1	12 ± 2	113 ± 9
	LBO	8.7 ± 0.4	8.7 ± 0.7	<D.L.	10 ± 1	116 ± 10

alkaline and moderately reducing waters enriched in carbonate, sulfate, and chloride, the adsorption of As onto Fe or Al oxides is unlikely, and As is thermodynamically found as a free As(V) ion (Stollenwerk, 2003). In addition, the relatively high phosphate and silica content (Table S4) may have enhanced As(V) mobility through competition for adsorption sites (Radu et al., 2005; So et al., 2012; Su and Puls, 2001). Although As concentrations were extremely high, we did not find any methylated As forms [i.e., DMAs(V) and MMAs(V)] in the surface water of all three lakes. As methylation is a microbial mechanism that has been linked to different environmental parameters such as high temperatures (Chen et al., 2021; Müller et al., 2022; Zhao et al., 2013), low redox conditions (Frohne et al., 2011; Mestrot et al., 2009), low pH (Baker et al., 1983; Müller et al., 2022; Wang et al., 2020; Zhao et al., 2013), and sulfate concentrations (Chen et al., 2021; Müller et al., 2022). While the redox conditions and sulfate concentrations in the lakes would enhance As methylation, low temperatures, and high pH would not favor it. Of course, the environmental conditions are only proxies for the microbial species present in the studied environment, and the absence of methylating microorganisms, those expressing the As(III) methyltransferase gene (*arsM),* would result in no methylation (Viacava et al., 2020).

Apart from surface waters, extreme As concentrations (As_{sed}) were also found in sediments of LV, reaching 6506 ± 307 mg kg^{-1}. As_{sed} were, however, lower in LC, i.e., 267 ± 62 mg kg^{-1}. Only 0.2 to 1 % of As was found associated with AVS at LC and LV, showing that As was weakly associated with reduced sulfur forms (e.g., mackinawite) and poorly crystalline Fe-Al (hydr)oxides (Table S8). Unfortunately, total Fe or S concentrations were not measured in these sediments. Still, one can speculate that, in such sulfate-rich sediments with active sulfate-reducing conditions, sulfur-bearing As phases such as realgar or orpiment are the most likely primary arsenic-bearing phases as observed for similar environments (Day et al., 2004; Khosravi et al., 2019; Ryu et al., 2002). In parallel, As concentrations in biomats collected on the shores of the lake Islands at LC showed values from 224 ± 5 to 1576 ± 19 mg kg^{-1} dw (Fig. S2), which are in the range of those reported in hyper-accumulating periphyton collected in Lake Titicaca [1452 ± 66 to 2647 ± 1263 mg As kg^{-1} dw (Sarret et al., 2019)].

In summary, As concentrations are high in the three studied lakes and are mainly encountered as free As(V) in surface waters, a highly available form for microorganisms (Roane et al., 2015), which may impact living organisms.

3.4. Lower methylmercury accumulation in the lake with increasing salinity

Total mercury concentrations in filtered (THg_F = 6.6 ± 2.3 ng L^{-1}) and unfiltered (THg_{UNF} = 34.5 ± 21.3 ng L^{-1}, average ± SD) waters (Fig. 4 a and b) were among the highest values reported in the Altiplano region including the most eutrophic areas of Lake Titicaca (Achá et al., 2018; Guédron et al., 2020b; Guédron et al., 2017a), the mine-contaminated Lake Uru-Uru (Alanoca et al., 2016b; Guédron et al., 2020a), and the Great Salt Lakes (Johnson et al., 2015; Peterson and Gustin, 2008). THg_{UNF} concentrations increased from LB to LV and LC (Fig. 4) following increasing DOC concentrations (R^2 = 0.96, $p < 0.01$, Fig. S3), and THg was mainly bound to suspended particles at LC (87 ± 7 %) and LV (84 ± 20 %), and a lesser extent at LB (63 ± 11 %). In contrast, $MMHg_{UNF}$ concentrations were at least 10-fold higher at LB

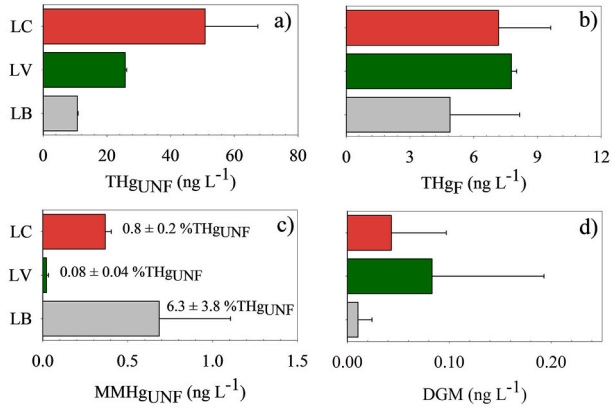

Fig. 4. Mercury distribution in surface water of Laguna Colorada (LC), Verde (LV), and Blanca (LB); total mercury in a) unfiltered and b) filtered water, c) monomethylmercury in unfiltered water, and d) dissolved gaseous mercury (DGM).

(0.69 ± 0.42 ng L^{-1}) and LC (0.37 ± 0.04 ng L^{-1}) than at LV (0.02 ± 0.01 ng L^{-1}) and represented respectively 6 ± 4 % of THg_{UNF} at LB, and below 1 % at LC (0.8 ± 0.2 %) and LV (0.08 ± 0.04 %). Such differences in Hg speciation between the 3 lakes likely result from the decrease in diversity and microbial activities with increasing salinity (Fig. S3), which was previously reported to impose constraints on *Hg*-methylating populations and to affect the availability of Hg(II) for methylation (Boyd et al., 2017). In addition, higher adsorption of inorganic Hg by algae [i.e., *Dunaliella* sp. (Fisher et al., 1984; Singh et al., 2019)] in the hypersaline LC might also restrict Hg availability for methylation.

In surface sediments, THg concentrations were relatively low compared to values reported in the Great salt lakes (Johnson et al., 2015) and at least 5 times higher at LC (62 ± 56 μg kg^{-1}) than at LB (12 ± 7 μg kg^{-1}) and LV (11 ± 6 μg kg^{-1}). MMHg never exceeded 1 % of THg (i.e., on average, MMHg = 0.5 ± 0.2 and 0.26 ± 0.04 μg kg^{-1}, at LC and LV, respectively). In biomats collected on the shores of LC, both THg concentrations and the percentage of MMHg were in the range of values measured in surface sediments (Fig. S2). This likely supports enhanced Hg scavenging onto OM and transfer to the sediment in the most productive lakes by *Dunaliella* green algae (Fisher et al., 1984; Singh et al., 2019).

3.5. Selenium speciation in lake water driven by primary productivity

Total selenium (TSe) concentrations in unfiltered surface water decreased from LC (2.5 ± 0.2 μg L^{-1}) to LV (0.9 ± 0.2 μg L^{-1}) and LB (0.26 ± 0.05 μg L^{-1}, Fig. 5).

The concentrations at LC and LV are in the range of reported values for contaminated waters (Luoma and Rainbow, 2008), and in the highest range of values reported in saline lakes like the Salton Sea [0.5 to 2 μg L^{-1} (Schroeder et al., 2002)], the Great Salt lake [0.3 to 1 μg L^{-1} (Diaz et al., 2009)], and 16 freshwater lakes from mining areas in Canada [0.035 to 3.1 μg·L^{-1} (Ponton and Hare, 2013)]. Selenium likely originates from the erosion of volcanic rock in the South Lipez, and thus, Se inputs to the lakes probably occur dominantly as selenate (Floor et al.,

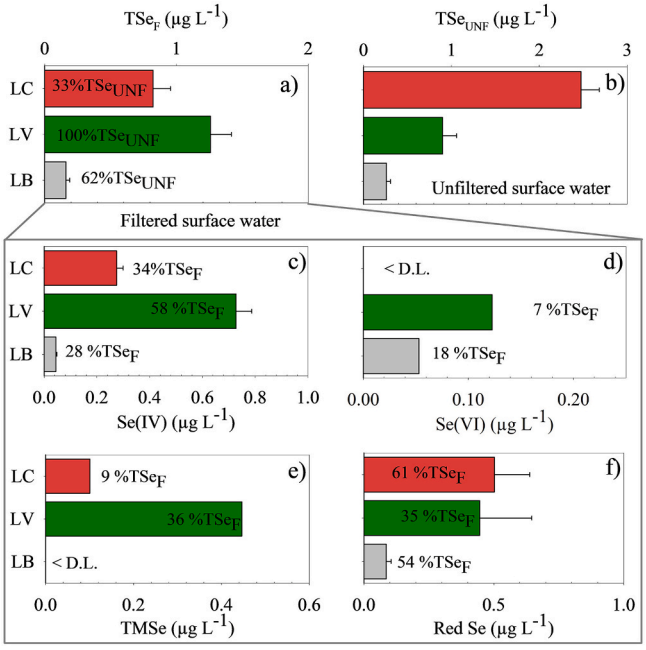

Fig. 5. Total selenium concentration in a) filtered and b) unfiltered surface water of Laguna Colorada (LC), Verde (LV), and Blanca (LB). Percentages in the bars indicate the respective average percentage of SeF in the UNF fraction. Bottom panel: Se speciation in filtered water with the respective average percentage of Se_F, for c) selenite [Se(IV)], d) Se (VI), e) trimethyl selenonium (TMSe), and f) reduced selenium (Red.Se). (For interpretation of the references to colour in this figure legend, the reader is referred to the web version of this article.)

2011; Winkel et al., 2012). The partitioning of Se differed between lakes with a higher partitioning onto solid phase in the most productive lakes LC ($TSe_F = 33 \pm 5$ %) and LB ($TSe_F = 62 \pm 8$ %), whereas at LV, 100 % of TSe was in the filtered (dissolved) fraction (Fig. 5). Such difference in Se partitioning in surface water likely results from changes in the OM binding capacity and Se speciation in relation with the lake's physico-chemical characteristics and biological activities (Nancharaiah and Lens, 2015).

At LC, Se in the filtered water was dominantly found as reduced Se species [i.e., Red.Se = organic Se(-II) + Se(0) ≈ 61 ± 16 %, Fig. 5] and as selenite [Se(IV) ≈ 34 ± 6 %]. Se(VI) was not detected, and the concentrations of the organic Se form trimethyl selenonium were close to quantification limits (TMSe ≈ 9 ± 6 %), meaning that the Red.Se pools included organic Se compounds or elemental Se(0) nanoparticles that did not elute out of our chromatographic separation. In contrast, Se speciation at LV was dominated by selenite [Se(IV) = 58 ± 9 %] and trimethyl selenonium (TMSe = 36 ± 5 %) in the oxygenated surface water. At LV, the Red.Se pool (35 ± 15 %) was thus mainly composed of TMSe. At LB, TMSe was not detected, and Se was mostly found as selenite and Red.Se, as in lake LV, but with reversed proportions, i.e., higher proportions of Red.Se (54 ± 15 %) than selenite (28 ± 6 %). Selenate was detected in one sample out of two in these two lakes, resulting in marginal proportions of this most oxidized Se species (on average, 18 ± 12 and 7 ± 4 % at LB and LV, respectively). Hence, the surface waters decreased in oxidized Se forms (i.e., selenate and selenite) from LV to LB and to LC, which may be related to increased Se reduction by sulfate-reducing bacteria in lakes enriched in OM, and where the installation of reducing conditions is favored (Nancharaiah and Lens, 2015). Consistently, higher partitioning of Se onto organic-rich suspended solids results from adsorption onto OM-rich suspended solids and algal (e.g., *Dunaliella*) Se uptake (Reunova et al., 2007; Singh et al., 2023; Yamaoka et al., 1990). This is consistent with the high TSe content in biomats at LC ranging from below 50 to 767 ± 33 µg g^{-1} dw (Fig. S2). In opposition to unfiltered surface water, the highest total selenium (TSe) concentrations in surface sediments were found at LV (261 ± 13 µg kg^{-1}) and the lowest at LC (141 ± 67 µg kg^{-1}). These concentrations are in the mid-lower range of worldwide Se content in sedimentary rock [0.01–7.0 mg kg^{-1} (WHO, 1987)] or in saline lake sediment like the Salton Sea [i.e., 0.2 to 2.9 mg kg^{-1} (Schroeder et al., 2002)]. Similar to As, the higher Se content in the sediment of the most saline LV lake suggests a higher contribution of inorganic carrier phases (e.g., carbonates) in the adsorption of Se (Wang and Gao, 2001). In contrast, concentrations decrease for Hg, which has only a low affinity for these phases.

3.6. *Lagunas Colorada and Verde as sources of volatile Hg and Se to the atmosphere*

Volatile As compounds in air were below the detection limit of the chemotrapping method we used (i.e., below 77 ng m^{-3}) at the three studied lakes. This supports that even in the most productive and relatively N- and P-rich lake LC, As methylation and volatilization by freshwater micro-organisms were not a significant route of detoxification for living organisms (Mestrot et al., 2013). This also confirms recent findings showing that organisms harboring an efficient As(III) efflux system do not drive As methylation, which probably serves a primary function other than detoxification in anaerobes (Viacava et al., 2020).

Total gaseous Hg concentrations (TGM) in the air were also low at the less productive LV and LB lakes (1.3 ± 0.7 ng m^{-3}) and the more productive LC lake (1.4 ± 0.6 ng m^{-3}; Fig. 6a). They were within the regional background levels [1.1 ± 0.2 ng m^{-3} (Guédron et al., 2017a)] and similar to the TGM concentrations reported for Great Salt Lakes (Peterson and Gustin, 2008).

In all three lakes, DMHg measurements in water and air samples were found below the detection limit of the chemotrapping method (ca. 0.01 pg L^{-1} and 0.3 pg m^{-3} for water and air samples, respectively). Thus, gaseous elemental mercury (GEM) remained the main contributor to both the DGM and TGM. This finding is also consistent with the reducing conditions monitored in the lakes and the previous discussion on the MMHg distribution in water. Moreover, the three lakes' surface waters were supersaturated with gaseous Hg, with DGM concentrations reaching 161, 83, and 20 pg L^{-1} in LV, LC, and LB surface water, respectively.

There was thus a net evasion flux of mercury to the atmosphere with average fluxes densities (FD) three to eight times higher at LV (957 ng m^{-2} d^{-1}) than at LC (314 ± 132 ng m^{-2} d^{-1}) and LB (96 ng m^{-2} d^{-1}), showing that the yields of Hg reduction and release to the atmosphere increased with increasing salinity rather than productivity (Fig. 6). In these high altitude lakes, intense UV-A and visible radiation [i.e.; averaging annually between 200 and 400 W.m^{-2} (Alanoca et al., 2016a; Bouchet et al., 2022)] are favorable for the photo-mediated reduction of Hg(II) to Hg(0) in waters with high concentrations of DOC (Amyot et al., 1997; Amyot et al., 1994). On the other hand, the higher DGM fluxes at LC than LB could reflect higher biological Hg reduction (Siciliano and Lean, 2002; Vandal et al., 1991) at LC and may involve microbes that expressed the merA gene (Barkay et al., 1989) and potentially phototrophic organisms, such as algae [e.g., *Chlorella*, (Poulain et al., 2004)]. When the DGM fluxes are extrapolated to the lake area, our dataset indicates annual emissions of 1.0 kg y^{-1} at LB, 6.0 kg y^{-1} at LC, and 5.6 kg y^{-1} at LV.

As for Hg, significant concentrations of volatile Se were detected in water (Fig. 6b), whereas they were low in air samples and close to the detection limit of the analytical method. Background atmospheric concentrations average 0.012 ± 0.008 ng m^{-3} for LV and LB and 0.014 ± 0.007 ng m^{-3} for LC. Unsurprisingly, the highest volatile Se concentrations in water were found at LC and were dominated by the species dimethylselenide (DMSe = 206.2 ± 1.3 ng m^{-3}) with traces of dimethylselenylsulphide (DMSSe = 5.0 ± 1.2 ng m^{-3}) and other unidentified species (XSe = 3.6 ± 0.2 ng m^{-3}). In contrast, only DMSe was detected

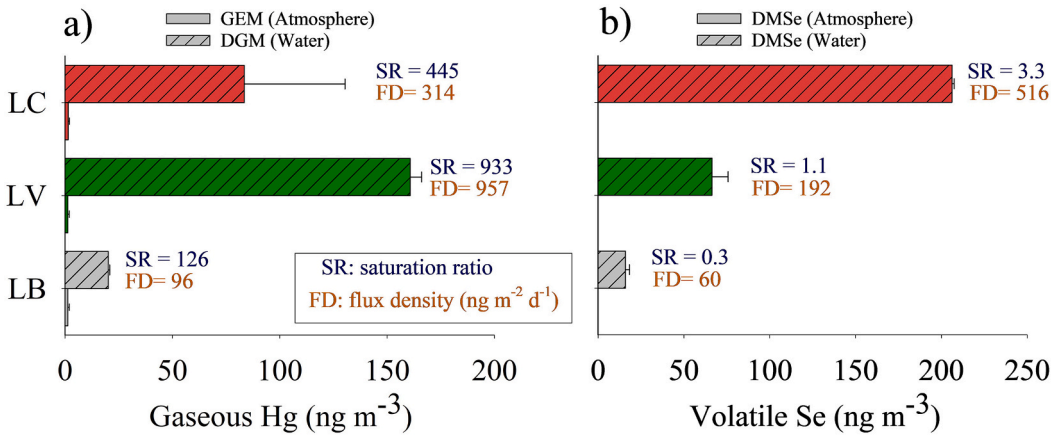

Fig. 6. a) Total gaseous mercury concentration in the air (gaseous elemental mercury; GEM) and water (dissolved gaseous mercury; DGM) and b) Total volatile selenium (dimethylselenide; DMSe) concentration in the air and water at Laguna Colorada (LC), Verde (LV) and Blanca (LB). Saturation ratio (SR) and flux density (FD).

in the waters of LV (66.4 ± 9.4 ng m^{-3}) and LB (16 ng m^{-3}). These values are much lower than the ones obtained in the nearby Lakes Poopo and Uru-Uru, where total volatile Se (TVSe) ranges were 1038–1740 and 42–1679 ng m^{-3}, respectively (Lanceleur et al., 2019). Calculated FD of water-air volatile Se exchanges confirmed that the eutrophic and reducing lake LC was a relatively important source of Se to the atmosphere (516 ± 2 ng m^{-2} d^{-1}). In contrast, the oligotrophic lake LV was a moderate source (192 ± 81 ng m^{-2} d^{-1}) and LB a low one (60 ng m^{-2} d^{-1}).

When the estimated volatile Se fluxes are extrapolated to the lake area, our dataset indicates annual emissions reaching 9.8 kg y^{-1} at LC and 1.1 and 0.7 kg y^{-1} at LV and LB. Such annual emissions of volatile Se at LC are an order of magnitude lower than those measured in the great salt lakes [1455 kg y^{-1} (Diaz et al., 2009)], and Lake Poopo (600 to 1000 kg y^{-1}) and Lake Uru-Uru [2 to 120 kg y^{-1} (Lanceleur et al., 2019)]. The ten times higher fluxes of volatile Se measured at LC compared to LV and LB are consistent with previous studies conducted in estuarine and saline environments, which showed that volatile methylated Se increased with decreasing salinity and increasing concentrations of phytoplankton and zooplankton (Diaz et al., 2009; Tessier et al., 2002). Hence, although more saline than LB, the highly productive LC is the main source of volatile Se species to the atmosphere.

4. Conclusions

Hypersaline lakes of the Altiplano are unique high-altitude ecosystems where extremophiles have adapted to the high insolation and exposure to high salinity and contaminant concentrations due to high water evaporation. In particular, extreme As concentrations in surface waters (up to ~80 mg L^{-1}) and sediments (up to 6.7 g kg^{-1}) were found in the three studied hypersaline Lakes, with declining As concentrations with increasing spring water inputs. Such spring sources are also suggested to favor the abundance and biological diversity (i.e., benthic biota, water birds…) through nutrient loads (e.g., phosphate and nitrate), favoring the biodilution of contaminants. In contrast, in hypersaline Lake weakly renewed by spring water inputs, high proportions of oxidized As and Se species in the dissolved phase result in low biodiversity or even a nearly absence of life. In the most productive lakes, the high biological productivity creates positive feedback through the scavenging of dissolved species, the reduction and/or methylation of Hg and Se, and subsequent volatilization to the atmosphere and/or export to the sediments.

This is the first study to provide information on total, dissolved species, and volatile species of As, Hg, and Se jointly in the high-altitude southern central Altiplano region. Further investigations must rely on the adaptative capacity and strategy of organisms living in these hypersaline lakes to assess the impact and defense mechanisms developed in such a toxic environment.

CRediT authorship contribution statement

Stéphane Guédron: Writing – review & editing, Writing – original draft, Validation, Supervision, Resources, Project administration, Methodology, Investigation, Funding acquisition, Formal analysis, Data curation, Conceptualization. **Julie Tolu:** Writing – review & editing, Validation, Resources, Methodology, Investigation, Formal analysis, Data curation. **David Amouroux:** Writing – review & editing, Validation, Supervision, Project administration, Investigation, Funding acquisition. **Emmanuel Tessier:** Writing – review & editing, Validation, Methodology, Investigation, Formal analysis, Data curation. **Carlos Molina:** Writing – review & editing, Resources, Methodology, Investigation, Formal analysis. **Maïté Bueno:** Writing – review & editing, Validation, Methodology, Formal analysis, Data curation. **Adrien Mestrot:** Writing – review & editing, Validation, Methodology, Formal analysis, Data curation. **Delphine Tisserand:** Methodology, Formal analysis. **Dario Acha:** Writing – review & editing, Validation, Supervision, Resources, Project administration, Methodology, Investigation, Funding acquisition, Formal analysis, Data curation.

Declaration of competing interest

The authors declare the following financial interests/personal relationships which may be considered as potential competing interests: Acha reports financial support was provided by Swiss Agency for Development and Cooperation. Amouroux financial support was provided by French National Research Agency. If there are other authors, they declare that they have no known competing financial interests or personal relationships that could have appeared to influence the work reported in this paper.

Data availability

All data are provided in supplementary tables

Acknowledgments

This work is a contribution to the “Identificación de Bioindicadores de cambio climático en lagos emblemáticos del Altiplano Boliviano” project [Proyecto de investigación aplicada para la adaptación al cambio climático (PIA-ACC, UMSA20: COSUDE)] founded by the Swiss

Cooperation and administrated by the Universidad Mayor de San Andres, PI: D. Acha: darioacha@yahoo.ca, LA PACHAMAMA project (ANR CESA program, No ANR-13-CESA-0015-01, PI: D. Amouroux: david.amouroux@univ-pau.fr), and the LMI ALTIPLANO (PIs: S. Guédron: stephane.guedron@ird.fr, and D. Acha: darioacha@yahoo.ca).

We wish to thank J. Gardon, A. Terrazas, C. Gonzalez, J.C. Salinas, A. Castillo, and M. Claure (IRD Bolivia) for their help and assistance during the field campaigns.

Appendix A. Supplementary data

Supplementary data to this article can be found online at https://doi.org/10.1016/j.gexplo.2024.107577.

References

Achá, D., et al., 2018. Algal bloom exacerbates hydrogen sulfide and methylmercury contamination in the emblematic high-altitude Lake Titicaca. Geosciences 8, 438.
Alanoca, L., et al., 2016a. Diurnal variability and biogeochemical reactivity of mercury species in an extreme high altitude lake ecosystem of the Bolivian Altiplano. Environ. Sci. Pollut. Res. 23 (7), 6919–6933.
Alanoca, L., et al., 2016b. Synergistic effects of mining and urban effluents on the level and distribution of methylmercury in a shallow aquatic ecosystem of the Bolivian Altiplano. Environ. Sci.: Processes Impacts 18 (12), 1550–1560.
Amouroux, D., Tessier, E., Pécheyran, C., Donard, O., 1998. Sampling and probing volatile metal (loid) species in natural waters by in-situ purge and cryogenic trapping followed by gas chromatography and inductively coupled plasma mass spectrometry (P-CT–GC–ICP/MS). Anal. Chim. Acta 377 (2–3), 241–254.
Amouroux, D., Wasserman, J.C., Tessier, E., Donard, O.F.X., 1999. Elemental mercury in the atmosphere of a tropical amazonian forest (French Guyana). Environ. Sci. Technol. 33 (17), 3044–3048.
Amyot, M., Mierle, G., Lean, D.R., McQueen, D.J., 1994. Sunlight-induced formation of dissolved gaseous mercury in lake waters. Environ. Sci. Technol. 28, 2366–2371.
Amyot, M., Mierle, G., Lean, D., McQueen, D.J., 1997. Effect of solar radiation on the formation of dissolved gaseus mercury in temperate lakes. Geochim. Cosmochim. Acta 61 (5), 975–987.
Angel, A., Vila, I., Herrera, V., 2016. Extremophiles: photosynthetic systems in a high-altitude saline basin (Altiplano, Chile). Int. Aquat. Res. 8, 91–108.
Arriaza, B., et al., 2009. Exploring chronic arsenic poisoning in pre-Columbian Chilean mummies. J. Archaeol. Sci. 37 (6), 1274–1278.
Bagnato, E., et al., 2014. Mercury fluxes from volcanic and geothermal sources: an update. Geol. Soc. Lond. Spec. Publ. 410 (1), 263–285.
Baker, M., Inniss, W., Mayfield, C., Wong, P., Chau, Y., 1983. Effect of pH on the methylation of mercury and arsenic by sediment microorganisms. Environ. Technol. 4 (2), 89–100.
Barkay, T., Liebert, C., Gillman, M., 1989. Environmental significance of the potential for mer(Tn21)-mediated reduction of Hg2+ to Hg0 in Natural waters. Appl. Environ. Microbiol. 55 (5), 1196–1202.
Bissen, M., Frimmel, F.H., 2003. Arsenic - a review. Part I: occurrence, toxicity, speciation, mobility. Acta Hydrochim. Hydrobiol. 31 (1), 9–18.
Bouchet, S., et al., 2011. Measurements of gaseous mercury exchanges at the sediment-water, water-atmosphere and sediment-atmosphere interfaces of a tidal environment (Arcachon Bay, France). J. Environ. Monit. 13, 1351.
Bouchet, S., et al., 2022. In situ photochemical transformation of Hg species and associated isotopic fractionation in the water column of high-altitude lakes from the Bolivian Altiplano. Environ. Sci. Technol. 56 (4), 2258–2268.
Bourrelly, P., 1966. Les Algues d'eau douce, initiation à la systématique. Faunes et flores actuelles, 1. N. Boubée, 567 pp.
Boyd, E.S., et al., 2017. Effect of salinity on mercury methylating benthic microbes and their activities in Great Salt Lake, Utah. Sci. Total Environ. 581, 495–506.
Bundschuh, J., et al., 2020. Arsenic in Latin America: new findings on source, mobilization and mobility in human environments in 20 countries based on decadal research 2010-2020. Crit. Rev. Environ. Sci. Technol. 1–139.
Cabrol, N.A., et al., 2009. The High-Lakes Project. J. Geophys. Res. Biogeosci. 114 (G2), G00D06.
Cadima, M., Fernandez, E., Lopez, L., 2005. Algas de Bolivia con énfasis en el Fitoplancton: Importancia, Ecología, Aplicaciones y Distribución de Géneros. Santa Cruz.
Caziani, S.M., et al., 2001. Waterbird richness in altiplano wetlands of northwestern Argentina. Waterbirds 103–117.
Chang, L.W., 1977. Neurotoxic effects of mercury–a review. Environ. Res. 14 (3), 329–373.
Chen, B., et al., 2013. Arsenic speciation in saliva of acute promyelocytic leukemia patients undergoing arsenic trioxide treatment. Anal. Bioanal. Chem. 405, 1903–1911.
Chen, C., et al., 2021. Sulfate addition and rising temperature promote arsenic methylation and the formation of methylated thioarsenates in paddy soils. Soil Biol. Biochem. 154, 108129.
Clarkson, T.W., Magos, L., 2006. The toxicology of mercury and its chemical compounds. Crit. Rev. Toxicol. 36 (8), 609–662.
Cline, J.D., 1969. Spectrophotometric determination of hydrogen sulfide in natural waters 1. Limnol. Oceanogr. 14 (3), 454–458.
Cockell, C.S., 2001. A Photobiological History of Earth, Ecosystems, Evolution, and Ultraviolet Radiation. Springer, pp. 1–35.
Day, P.A., Vlassopoulos, D., Root, R., Rivera, N., 2004. The influence of sulfur and iron on dissolved arsenic concentrations in the shallow subsurface under changing redox conditions. Proc. Natl. Acad. Sci. USA 101 (38), 13703.
De Loma, J., et al., 2019. Elevated arsenic exposure and efficient arsenic metabolism in indigenous women around Lake Poopo, Bolivia. Sci. Total Environ. 657, 179–186.
Dejoux, C., 1993. Benthic Invertebrates of Some Saline Lakes of the Sud Lipez Region, Bolivia, Saline Lakes V. Springer, pp. 257–267.
Díaz, C., Maidana, N., 2005. Diatomeas de los salares Atacama y Punta Negra, II Región. Centro de Ecología Aplicada Ltda, Santiago, Chile, Chile, p. 148.
Diaz, X., Johnson, W.P., Naftz, D.L., 2009. Selenium mass balance in the Great Salt Lake, Utah. Sci. Total Environ. 407 (7), 2333–2341.
Domínguez, E., Fernández, H.R., 2009. Macroinvertebrados bentónicos sudamericanos. Sistemática y biología. Fundación Miguel Lillo, Tucumán, Argentina, p. 656.
Dopp, E., Hartmann, L.M., Florea, A.M., Rettenmeier, A.W., Hirner, A.V., 2004. Environmental distribution, analysis, andtoxicity of organometal(loid) compounds. Crit. Rev. Toxicol. 34 (3), 301–333.
Duker, A.A., Carranza, E., Hale, M., 2005. Arsenic geochemistry and health. Environ. Int. 31 (5), 631–641.
Duval, B., et al., 2023. Dynamics, distribution, and transformations of mercury species from pyrenean high-altitude lakes. Environ. Res. 216, 114611.
Entwisle, T., Sonneman, J., Lewis, S., 1997. Freshwater Algae in Australia: A Guide to Conspicuous Genera, New South Wales, 242 pp.
Faith, D.P., 1992. Conservation evaluation and phylogenetic diversity. Biol. Conserv. 61 (1), 1–10.
Figueroa, Y.P., 2018. Geochemical and Isotopic Characteristics of the Laguna Colorada Geothermal Area – SW Bolivia. United Nation University, Orkustofnun, Grensasvegur 9, IS-108 Reykjavik, Iceland.
Fisher, N.S., Bohe, M., Teyssie, J.-L., 1984. Accumulation and toxicity of Cd, Zn, Ag, and Hg in four marine phytoplankters. In: Marine Ecology Progress Series. Oldendorf, 19 (3), pp. 201–213.
Fleming, E.D., Prufert-Bebout, L., 2010. Characterization of cyanobacterial communities from high-elevation lakes in the Bolivian Andes. J. Geophys. Res. Biogeosci. 115 (G2).
Floor, G.H., Román-Ross, G., 2012. Selenium in volcanic environments: a review. Appl. Geochem. 27 (3), 517–531.
Floor, G.H., Iglesías, M., Román-Ross, G., Corvini, P.F.X., Lenz, M., 2011. Selenium speciation in acidic environmental samples: application to acid rain–soil interaction at Mount Etna volcano. Chemosphere 84 (11), 1664–1670.
Frohne, T., Rinklebe, J., Diaz-Bone, R.A., Du Laing, G., 2011. Controlled variation of redox conditions in a floodplain soil: impact on metal mobilization and biomethylation of arsenic and antimony. Geoderma 160 (3–4), 414–424.
Gadd, G.M., 1993. Microbial formation and transformation of organometallic and organometalloid compounds. FEMS Microbiol. Rev. 11 (4), 297–316.
Guédron, S., et al., 2014. Baseline investigation of (methyl)mercury in waters, soils, sediments and key foodstuffs in the Lower Mekong Basin: the rapidly developing city of Vientiane (Lao PDR). J. Geochem. Explor. 143 (0), 96–102.
Guédron, S., et al., 2017a. Mercury contamination level and speciation inventory in the hydrosystem of Lake Titicaca: current status and future trends. Environ. Pollut. 231, 262–270.
Guédron, S., et al., 2017b. Late Holocene mercury deposition history in Lake Chungará (4500 m a.s.l., Chile): influence of volcanic eruptions and changes in paleolimnoecology. In: 13th International Conference on Mercury as a Global Pollutant. Providence, Rhode Island.
Guédron, S., et al., 2020a. Accumulation of methylmercury in the high-altitude Lake Uru Uru (3686 m asl, Bolivia) controlled by sediment efflux and photodegradation. Appl. Sci. 10 (21), 7936.
Guédron, S., et al., 2020b. Diagenetic production, accumulation and sediment-water exchanges of methylmercury in contrasted sediment facies of Lake Titicaca (Bolivia). Sci. Total Environ. 723, 138088.
Guédron, S., et al., 2021. Reconstructing two millennia of copper and silver metallurgy in the Lake Titicaca region (Bolivia/Peru) using trace metals and lead isotopic composition. Anthropocene 34, 100288.
Guédron, S., et al., 2023. Holocene variations in Lake Titicaca water level and their implications for sociopolitical developments in the central Andes. Proc. Natl. Acad. Sci. 120 (2), e2215882120.
Hammer, Ø., Harper, D.A., 2001. Past: paleontological statistics software package for educaton and data anlysis. Palaeontol. Electron. 4 (1), 1.
Hammer, Ø., Harper, D., Ryan, P., 2001. PAST: paquete de programas de estadística paleontológica para enseñanza y análisis de datos. Palaeontol. Electron. 4 (1), 4.
Heredia, C., et al., 2022. Anthropogenic eutrophication of Lake Titicaca (Bolivia) revealed by carbon and nitrogen stable isotopes fingerprinting. Sci. Total Environ. 845, 157286.
Holzinger, A., Pichrtová, M., 2016. Abiotic stress tolerance of charophyte green algae: new challenges for omics techniques. Front. Plant Sci. 7, 678.
Hurlbert, S.H., Chang, C.C.Y., 1984. Ancient ice islands in salt lakes of the Central Andes. Science 224 (4646), 299–302.
Hurlbert, S.H., Chang, C.C.Y., 1988. The Distribution, Structure, and Composition of Freshwater Ice Deposits in Bolivian Salt Lakes, Saline Lakes. Springer, pp. 271–299.
Hurlbert, S.H., Keith, J.O., 1979. Distribution and spatial patterning of flamingos in the Andean altiplano. Auk 96 (2), 328–342.
Hurlbert, S.H., Loayza, W., Moreno, T., 1986. Fish-flamingo-plankton interactions in the Peruvian Andes 1. Limnol. Oceanogr. 31 (3), 457–468.

Iltis, A., Risacher, F., Servant Vildary, S., 1984. Contribution à l'étude hydrobiologique des lacs salés du sud de l'Altiplano bolivien. Rev. Hydrobiol. Trop. 17 (3), 259–273.
Jellison, R., Anderson, R.F., Melack, J.M., Heil, D., 1996. Organic matter accumulation in sediments of hypersaline Mono Lake during a period of changing salinity. Limnol. Oceanogr. 41 (7), 1539–1544.
Johnson, W.P., et al., 2015. Total-and methyl-mercury concentrations and methylation rates across the freshwater to hypersaline continuum of the Great Salt Lake, Utah, USA. Sci. Total Environ. 511, 489–500.
Jones, M.T., Gislason, S.R., 2008. Rapid releases of metal salts and nutrients following the deposition of volcanic ash into aqueous environments. Geochim. Cosmochim. Acta 72 (15), 3661–3680.
Khosravi, R., Zarei, M., Vogel, H., Bigalke, M., 2019. Early diagenetic behavior of arsenic in the sediment of the hypersaline Maharlu Lake, southern Iran. Chemosphere 237, 124465.
Kleindienst, A., et al., 2023. Assessing comparability and uncertainty of analytical methods for methylated mercury species in seawater. Anal. Chim. Acta 1278, 341735.
Klindworth, A., et al., 2013. Evaluation of general 16S ribosomal RNA gene PCR primers for classical and next-generation sequencing-based diversity studies. Nucleic Acids Res. 41 (1), e1.
Lanceleur, L., et al., 2019. Cycling and atmospheric exchanges of selenium in Canadian subarctic thermokarst ponds. Biogeochemistry 145 (1–2), 193–211.
Lopez, R.P., Zambrana-Torrelio, C., 2006. Representation of Andean dry ecoregions in the protected areas of Bolivia: the situation in relation to the new phytogeographical findings. Biodivers. Conserv. 15 (7), 2163–2175.
Luoma, S.N., Rainbow, P.S., 2008. Metal Contamination in Aquatic Environments: Science and Lateral Management. Cambridge university press.
Maier, K.J., Knight, A.W., 1994. Ecotoxicology of selenium in freshwater systems. In: Reviews of Environmental Contamination and Toxicology: Continuation of Residue Reviews, pp. 31–48.
Mandal, B.K., Suzuki, K.T., 2002. Arsenic round the world: a review. Talanta 58 (1), 201–235.
Merritt, R.W., Cummins, K.W., 1996. An Introduction to the Aquatic Insects of North America. Kendall Hunt, Dubuque, p. 862.
Mestrot, A., et al., 2009. Quantitative and qualitative trapping of arsines deployed to assess loss of volatile arsenic from paddy soil. Environ. Sci. Technol. 43 (21), 8270–8275.
Mestrot, A., et al., 2011. Field fluxes and speciation of arsines emanating from soils. Environ. Sci. Technol. 45 (5), 1798–1804.
Mestrot, A., Planer-Friedrich, B., Feldmann, J., 2013. Biovolatilisation: a poorly studied pathway of the arsenic biogeochemical cycle. Environ. Sci.: Processes Impacts 15 (9), 1639–1651.
MMAyA, 2016. Análisis e interpretación de resultados de la expedición científica de evaluación de las características limnológicas y ecológicas de. Lago Menor del Titicaca.
Monperrus, M., Tessier, E., Veschambre, S., Amouroux, D., Donard, O., 2005. Simultaneous speciation of mercury and butyltin compounds in natural waters and snow by propylation and species-specific isotope dilution mass spectrometry analysis. Anal. Bioanal. Chem. 381 (4), 854–862.
Monperrus, M., Gonzalez, P.R., Amouroux, D., Alonso, J.I.G., Donard, O.F.X., 2008. Evaluating the potential and limitations of double-spiking species-specific isotope dilution analysis for the accurate quantification of mercury species in different environmental matrices. Anal. Bioanal. Chem. 390 (2), 655–666.
Müller, V., Chavez-Capilla, T., Feldmann, J., Mestrot, A., 2022. Increasing temperature and flooding enhance arsenic release and biotransformations in Swiss soils. Sci. Total Environ. 838, 156049.
Nancharaiah, Y.V., Lens, P., 2015. Ecology and biotechnology of selenium-respiring bacteria. Microbiol. Mol. Biol. Rev. 79 (1), 61–80.
Nightingale, P.D., et al., 2000. In situ evaluation of air-sea gas exchange parameterizations using novel conservative and volatile tracers. Glob. Biogeochem. Cycles 14 (1), 373–387.
Nriagu, J., Becker, C., 2003. Volcanic emissions of mercury to the atmosphere: global and regional inventories. Sci. Total Environ. 304 (1–3), 3–12.
Ormachea Munoz, M., et al., 2013. Geogenic arsenic and other trace elements in the shallow hydrogeologic system of Southern Poopo Basin, Bolivian Altiplano. J. Hazard. Mater. 262, 924–940.
Peterson, C., Gustin, M., 2008. Mercury in the air, water and biota at the Great Salt Lake (Utah, USA). Sci. Total Environ. 405 (1–3), 255–268.
Pfister, L., et al., 2017. Terrestrial diatoms as tracers in catchment hydrology: a review. Wiley Interdiscip. Rev. Water 4 (6), e1241.
Ponton, D.E., Hare, L., 2013. Relating selenium concentrations in a planktivore to selenium speciation in lakewater. Environ. Pollut. 176, 254–260.
Poulain, A., et al., 2004. Biological and photochemical production of dissolved gaseous mercury in a boreal lake. Limnol. Oceanogr. 49 (6), 2265–2275.
Radu, T., Subacz, J.L., Phillippi, J.M., Barnett, M.O., 2005. Effects of dissolved carbonate on arsenic adsorption and mobility. Environ. Sci. Technol. 39 (20), 7875–7882.
Ramos Ramos, O.E., et al., 2012. Sources and behavior of arsenic and trace elements in groundwater and surface water in the Poopo Lake Basin, Bolivian Altiplano. Environ. Earth Sci. 66 (3), 793–807.
Ramos Ramos, O.E., et al., 2014. Geochemical processes controlling mobilization of arsenic and trace elements in shallow aquifers and surface waters in the Antequera and Poopo mining regions, Bolivian Altiplano. J. Hydrol. 518, 421–433.
Reunova, Y.A., Aizdaicher, N., Khristoforova, N., Reunov, A., 2007. Effects of selenium on growth and ultrastructure of the marine unicellular alga Dunaliella salina (Chlorophyta). Russ. J. Mar. Biol. 33, 125–132.
Risacher, F., Fritz, B., 1992. Mise en évidence d'une phase climatique holocène extrêmement aride dans l'Altiplano central, par la présence de la polyhalite dans le salar de Uyuni (Bolivie). CR Acad. Sci. Paris 314, 1371–1377.
Risacher, F.o., Fritz, B., 1991. Quaternary geochemical evolution of the salars of Uyuni and Coipasa, central Altiplano, Bolivia. Chem. Geol. 90 (3), 211–231.
Roane, T.M., Pepper, I.L., Gentry, T.J., 2015. Microorganisms and metal pollutants. In: Environmental Microbiology. Elsevier, pp. 415–439.
Rohn, I., et al., 2018. Selenium species-dependent toxicity, bioavailability and metabolic transformations in Caenorhabditis elegans. Metallomics 10 (6), 818–827.
Roulier, M., et al., 2021. Atmospheric iodine, selenium and caesium depositions in France: I. Spatial and seasonal variations. Chemosphere 273, 128971.
Ryu, J.-h., Gao, S., Dahlgren, R.A., Zierenberg, R.A., 2002. Arsenic distribution, speciation and solubility in shallow groundwater of Owens Dry Lake, California. Geochim. Cosmochim. Acta 66 (17), 2981–2994.
Sarret, G., et al., 2019. Extreme arsenic bioaccumulation factor variability in Lake Titicaca, Bolivia. Sci. Rep. 9 (1), 10626.
Scandiffio, G., Alvarez, M., 1992. Geochemical Report on the Laguna Colorada Geothermal Area, Bolivia. IAEA, Vienna, Austria.
Schroeder, R.A., Orem, W.H., Kharaka, Y.K., 2002. Chemical Evolution of the Salton Sea, California: Nutrient and Selenium Dynamics, The Salton Sea. Springer, pp. 23–45.
Schwarzenbach, R.P., Gschwend, P.M., Imboden, D.M., 2016. Environmental Organic Chemistry. John Wiley & Sons.
Segata, N., et al., 2011. Metagenomic biomarker discovery and explanation. Genome Biol. 12, 1–18.
Servant-Vildary, S., Risacher, F.o., Roux, M., 2002. Diatom based transfer function for estimating the chemical composition of fossil water. Calibration based on salt lakes of the Lipez area in the southwestern Bolivian Altiplano. In: Carnets de Géologie (M01-en), pp. 1–36.
Sharif, A., et al., 2013. Comparison of different air–water gas exchange models to determine gaseous mercury evasion from different European coastal lagoons and estuaries. Water Air Soil Pollut. 224, 1–16.
Siciliano, S.D., Lean, D.R.S., 2002. Methyltransferase: an enzyme assay for microbial methylmercury formation in acidic soils and sediments. Environ. Toxicol. Chem. 21 (6), 1184–1190.
Singh, A.K., et al., 2019. One pot hydrothermal synthesis of fluorescent NP-carbon dots derived from Dunaliella salina biomass and its application in on-off sensing of Hg (II), Cr (VI) and live cell imaging. J. Photochem. Photobiol. A Chem. 376, 63–72.
Singh, P., et al., 2023. Bioaccumulation of selenium in halotolerant microalga Dunaliella salina and its impact on photosynthesis, reactive oxygen species, antioxidative enzymes, and neutral lipids. Mar. Pollut. Bull. 190, 114842.
So, H.U., Postma, D., Jakobsen, R., Larsen, F., 2012. Competitive adsorption of arsenate and phosphate onto calcite; experimental results and modeling with CCM and CD-MUSIC. Geochim. Cosmochim. Acta 93, 1–13.
Stollenwerk, K.G., 2003. Geochemical Processes Controlling Transport of Arsenic in Groundwater: A Review of Adsorption, Arsenic in Ground Water. Springer, pp. 67–100.
Su, C., Puls, R.W., 2001. Arsenate and arsenite removal by zerovalent iron: effects of phosphate, silicate, carbonate, borate, sulfate, chromate, molybdate, and nitrate, relative to chloride. Environ. Sci. Technol. 35 (22), 4562–4568.
Tapia, J., Murray, J., Ormachea, M., Tirado, N., Nordstrom, D.K., 2019. Origin, distribution, and geochemistry of arsenic in the Altiplano-Puna plateau of Argentina, Bolivia, Chile, and Peru. Sci. Total Environ. 678, 309–325.
Tessier, E., Amouroux, D., Abril, G., Lemaire, E., Donard, O.F.X., 2002. Formation and volatilisation of alkyl-iodidesand -selenides in macrotidal estuaries. Biogeochemistry 59 (1), 183–206.
Tisserand, D., Guédron, S., Razimbaud, S., Findling, N., Charlet, L., 2021. Acid volatile sulfides and simultaneously extracted metals: a new miniaturized 'purge and trap' system for laboratory and field measurements. Talanta 122490.
Vandal, G.M., Mason, R.P., Fitzgerald, W.F., 1991. Cycling of volatile mercury in temperate lakes. Water Air Soil Pollut. 56, 791–803.
Viacava, K., et al., 2020. Variability in arsenic methylation efficiency across aerobic and anaerobic microorganisms. Environ. Sci. Technol. 54 (22), 14343–14351.
Wang, J., et al., 2020. Thiolated arsenic species observed in rice paddy pore waters. Nat. Geosci. 13 (4), 282–287.
Wang, W.-X., Wong, R.S., Wang, J., Yen, Y.-f., 2004. Influences of different selenium species on the uptake and assimilation of Hg (II) and methylmercury by diatoms and green mussels. Aquat. Toxicol. 68 (1), 39–50.
Wang, Z., Gao, Y., 2001. Biogeochemical cycling of selenium in Chinese environments. Appl. Geochem. 16 (11–12), 1345–1351.
Wehr, J.D., 2003. Freshwater habitats of algae. In: Freshwater Algae of North America-Ecology and Classification, pp. 11–57.
WHO, 1987. Environmental Health Criteria 58: Selenium.
Williams, W.D., Carrick, T.R., Bayly, I.A.E., Green, J., Herbst, D.B., 1995. Invertebrates in salt lakes of the Bolivian Altiplano. Int . J. Salt Lake Res. 4 (1), 65–77.
Winkel, L.H.E., et al., 2012. Environmental selenium research: from microscopic processes to global understanding. Environ. Sci. Technol. 46 (2), 571–579.
Yamaoka, Y., Takimura, O., Fuse, H., Kamimura, K., 1990. Accumulation of arsenic and selenium by Dunaliella sp. Appl. Organomet. Chem. 4 (3), 261–264.
Yoon, S.-H., et al., 2017. Introducing EzBioCloud: a taxonomically united database of 16S rRNA gene sequences and whole-genome assemblies. Int. J. Syst. Evol. Microbiol. 67 (5), 1613.
Zhao, F.-J., et al., 2013. Arsenic methylation in soils and its relationship with microbial arsM abundance and diversity, and As speciation in rice. Environ. Sci. Technol. 47 (13), 7147–7154.
Zwolak, I., Zaporowska, H., 2012. Selenium interactions and toxicity: a review. Cell Biol. Toxicol. 28 (1), 31–46.